Modelling of Materials for Silicon-Compatible Microelectronics

J. Dabrowski, G. Kissinger, G. Lippert, G. Lupina, M. Lukosius, P. Sana, T. Schroeder

published in

NIC Symposium 2018
K. Binder, M. Müller, A. Trautmann (Editors)

Forschungszentrum Jülich GmbH,
John von Neumann Institute for Computing (NIC),
Schriften des Forschungszentrums Jülich, NIC Series, Vol. 49,
ISBN 978-3-95806-285-6, pp. 239.
http://hdl.handle.net/2128/17544

© 2018 by Forschungszentrum Jülich
Permission to make digital or hard copies of portions of this work for personal or classroom use is granted provided that the copies are not made or distributed for profit or commercial advantage and that copies bear this notice and the full citation on the first page. To copy otherwise requires prior specific permission by the publisher mentioned above.

Modelling of Materials for Silicon-Compatible Microelectronics

Jarek Dabrowski, Gudrun Kissinger, Gunther Lippert, Grzegorz Lupina, Mindaugas Lukosius, Prabha Sana, and Thomas Schroeder

IHP, Im Technologiepark 25, 15236 Frankfurt (Oder), Germany
E-mail: dabrowski@ihp-microelectronics.com

Ab initio density functional theory (DFT) is an established method to model the behaviour of materials at the atomic scale. At the IHP, we use it to investigate materials systems that are of interest to the most popular and cost-efficient technology, by which electronics is made today: the silicon technology. Here we report on the results obtained for various materials: (a) for strictly 2D atomic sheets (graphene), (b) for heteroepitaxial layers (oxides and nitrides), their surfaces, and the interfaces between these films, and (c) for bulk crystals (defects in silicon). The graphene sheets are intended as components of chemical sensors, optical modulators, and high-speed and high-power transistors. The chemical reactions and diffusion processes governing the nucleation and growth of graphene on perfect (flat and stepped) and defected surfaces of germanium films were simulated, and the mechanisms responsible for the observed growth modes were elucidated. The Sc oxide and nitride films constitute the topmost part of a heterostructure on which GaN diodes, lasers, and high-power transistors can be assembled. The simulations provided insight into the intermixing of oxygen and nitrogen. The substrate on which all these films and other device structures are grown, is crystalline silicon. For numerous applications it is critical that the substrate getters (collects and binds) the impurities that are unintentionally introduced by the technological process. The formation of oxygen precipitates used as the gettering centres is associated with the presence of missing atoms (vacancies) in the Si bulk. We studied the process of vacancy clustering and oxidation, we extrapolated the clustering results to infinite separation between the defects, and we discussed the implications also for the interpretation of deep level transient spectroscopy (DLTS) or for the strategy to perform numerically expensive defect calculations (as done with hybrid potentials), among others.

1 Introduction

IHP is a Leibniz Institute developing silicon-based technologies, circuits and systems for high-frequency applications in areas such as telecommunication, automation, and security. For this purpose, it combines basic and applied research. We report on selected results of *ab initio* density functional theory (DFT) calculations performed on the JURECA cluster to guide and to interpret the experiments being conducted at the Materials Department of the IHP. Three different fields are covered by this overview: (1) nucleation and growth of graphene films on Ge substrates[1–3], (2) growth of Sc nitride films on Sc oxide substrates[4], and (3) clustering of vacancies and oxygen in Si crystals[5,6].

Graphene is a monatomic sheet of sp^2-bonded carbon atoms. If successfully combined with the traditional silicon technology used nowadays for inexpensive microelectronics, graphene with its peculiar properties like the linear energy-momentum dependence of its charge carriers in a wide range of energies or its low sheet resistance in conjunction with its extreme thinness may enable mass production of circuits working at terahertz speed and of other useful components, like efficient on-chip optical modulators or precise chemical sensors. The formation of stable Si–C bonds hinders the growth of monolayer graphene directly on silicon wafers. Although graphene can be grown on a metal and then transferred

to Si or formed from SiC crystals produced on Si, technological constraints both make these approaches difficult to integrate with the established methods to fabricate Si-based chips. This is mostly due to the risk of contamination with metal atoms during transfer and to high temperatures when SiC is involved. A prospective solution is to grow graphene on germanium. Good graphene films can be obtained in this way and used either for transfer or for direct production of devices. On the way to the production line there are however still several challenges, which call for fundamental research that would expand our basic knowledge on the physical mechanisms governing the growth process. This is illustrated in Sec. 3, where reasons for the differences on the growth mode between various deposition methods are addressed.

Another way to enhance the value of Si microelectronics is to integrate it with the III-V materials known for their good performance in optoelectronics and high-power electronics. GaN belongs to this class. The integration is however hindered, e.g. by huge lattice mismatch and thermal between Si and GaN, so that a buffer layer separating both materials is required. This buffer must contain the misfit dislocations and other defects generated during the growth and the subsequent cooling, must separate Si and GaN chemically, and high grade GaN must be able to be grown on it. A prospective buffer is a $Si/Y_2O_3/Sc_2O_3/ScN$ stack. We used DFT to address several aspects of the growth of ScN films on Sc_2O_3, including the interface formation (influences the polarity of ScN and hence the polarity and quality of GaN), the layer stacking (influences planar defects in ScN), and intermixing (influences the contamination of GaN by O). These subjects are covered by Sec. 4.

A common denominator of these materials systems is the crystalline Si wafer, onto which the Ge and Y_2O_3 films are deposited. The bulk of the wafer contains oxygen stemming from the Si melt, from which the Si ingot was grown. Oxygen precipitates are useful, because they act as sinks for metal impurities, but their presence can interfere with the operation of devices, therefore their distribution must be controlled. This can be done inexpensively by taking advantage of the influence of Si vacancies on the precipitation of interstitial oxygen. Sec. 5 is devoted to the formation and oxidation of vacancy clusters.

2 Approach

DFT calculations are done with the tools provided by the Quantum Espresso package designed for massively parallel computations[8]. Atomic structures are optimised and the electronic structures are obtained by the pw.x utility, and energy barriers for structural transformations are computed by the neb.x utility. Plane wave basis set and pseudopotentials are used. The exchange-correlation energy is approximated by the gradient-corrected PBE functional and in special cases by the hybrid HSE06 functional. Van der Waals forces are treated within the semi-empirical DFT-D extension of DFT or as non-local DFT (rVV10).

3 Graphene on Ge(001)

Graphene can be grown on Ge by direct evaporation of C atoms in ultra-high vacuum (UHV) in a molecular beam epitaxy (MBE) chamber[1,2] or by exposing the substrate to a hydrocarbon flow in a chemical vapour deposition (CVD) chamber[2,3]. The flow usually contains H_2 and the pressure in the chamber may vary from high vacuum to atmospheric.

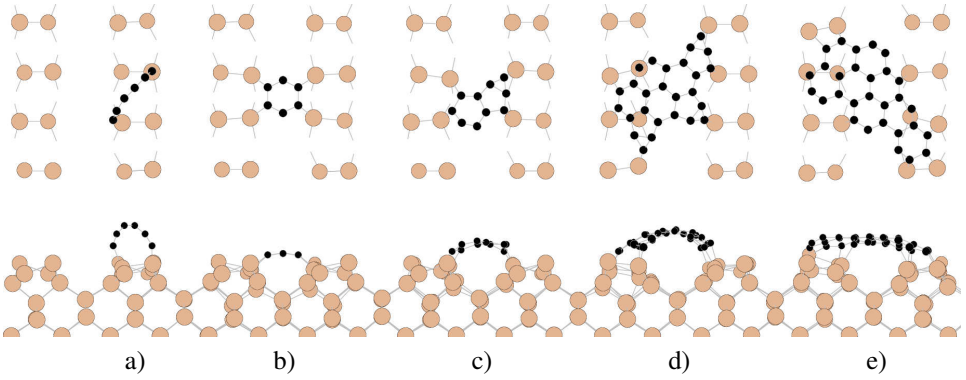

Figure 1. Carbon clusters on Ge(001); top and side views. C atoms are black. (a) C_6 string on top of a Ge dimer row. (b) C_6 ring between two Ge dimer rows. (c) C_{12}, two rings. (d) C_{26} cluster consisting of seven rings and bonded by seven Ge atoms from two neighbouring dimer rows. (e) C_{29} cluster with eight fully formed rings.

High vacuum experiments are easier to interpret, because the reactions begin on the substrate surface, while in the other case they are initiated in a hot gaseous layer above it. We apply all three deposition methods and we use Ge(001) films as the substrate.

From the experimental data it follows that hydrogen is needed to obtain monolayer graphene of at least acceptable quality. This can be understood on the basis of the calculations. Consider the Ge(001) surface[1,2]. The deposited C atoms diffuse on the surface or directly under it. When they meet one another, they have a tendency to form C strings (Fig. 1a) instead of the hexagonal rings (Fig. 1b) from which graphene is built. Many mobile, sticky strings consisting of several C atoms are thus produced on the surface. Hexagonal rings become stabilised in a C_{12} cluster (Fig. 1c), which is by 1.7 eV more stable than two C_6 strings. When the seeds grow, they remain attached to the substrate through C–Ge bonds (Fig. 1d-e). There are many relative orientations of the seed and the substrate. When the seeds turn into small graphene crystallites, these bonds prevent the crystallites from fully adjusting their relative position and orientation. Strain builds up in this way and defect formation in the graphene layer is promoted. For example, the carbon strings may form bridges between the neighbouring flakes and/or numerous orientational domains are created. Graphene flakes of useful size may grow only on top of such a highly disordered layer; in other words, MBE graphene is separated from Ge(001) by an interfacial layer that may resemble graphene locally but is highly disordered and defected.

The situation improves when H is available during the nucleation phase[2,3]. H atoms promote the formation of hexagonal C rings. Another beneficial action of H is that H attacks the bonds between Ge and C. A seed with its edge largely passivated by H becomes mobile, it can adjust itself better to the substrate and, as it becomes a crystallite, also to another crystallite. Furthermore, no C strings are there to bridge the crystallites.

When the surface coverage by H is only moderate, the surface defects known as Ge dimer vacancies (DV) play a role as nucleation centres: a C ring may be assembled (as C_8H_6, for example) and trapped there[2]. Graphene can nucleate also on the perfect surface, by polymerisation of hydrocarbon rings standing on Ge dimers (Fig. 2a)[2]. The rings can polymerise easily along (110), i.e., across the dimer rows. But to maintain low strain,

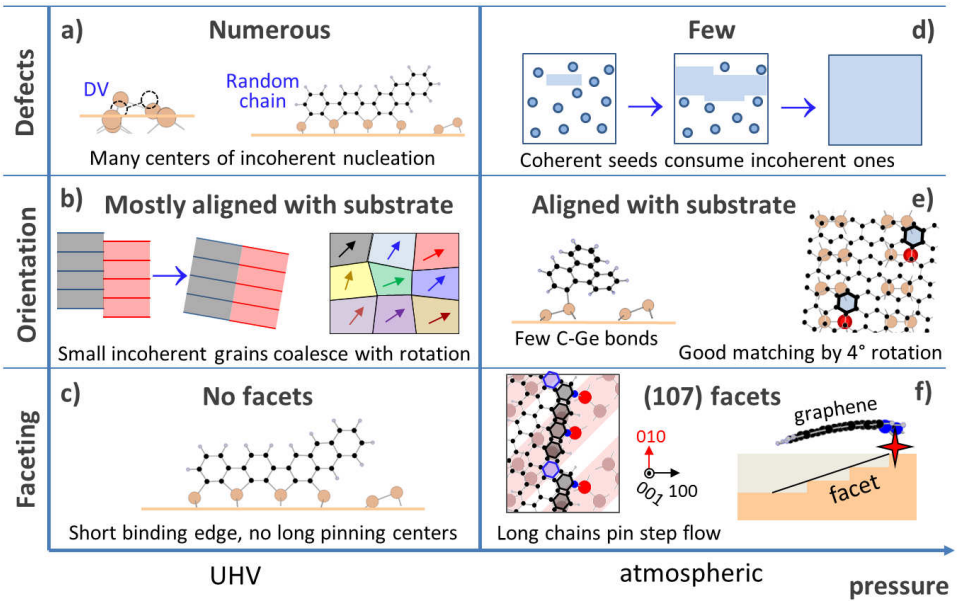

Figure 2. Growth modes of CVD Ge(001) graphene. UHV conditions may correspond, e.g., to 10^{-2} mbar of C_2H_4 at 930°C. (a) Low H coverage in the nucleation phase: many centres of incoherent nucleation. (b) The crystallites grow small and similar in size, so when two of them coalesce, they compete for the orientation: orientational disorder appears. (c) The bonds between the seeds and the substrate do not act as efficient pinning centres for surface steps, so that no surface facets form. (d) When the H coverage is high (like in the atmospheric regime, C_2H_4 precursor at 930°C), coherent seeds may form, grow fast and consume the small, slowly growing incoherent seeds. (e) The seeds may become coherent because H reduces the number of C–Ge bonds, so that the seeds may rotate easily. Graphene with C–C bonds rotated by 4° with respect to Ge dimer rows is nearly lattice-matched to Ge(001). (f) The rotated seeds expand easily along (010), pining the step flow: facets appear.

such polymer chains begin to avoid bonding with Ge when they are longer than three rings (Fig. 2a)[2], and soon it is faster to nucleate new seeds than to expand the existing ones. H is thus needed for the excess of polymers to become detached from the surface and to evaporate. Otherwise, numerous incoherent seeds are created and the graphene sheet consists of small grains, many of which coalesce with rotation (Fig. 2b). Significant orientational disorder appears (Fig. 2a-c), although some orientational correlation with Ge(001) prevails[2].

The detachment probability increases with increasing H coverage, but decreases with increasing number of C–Ge bonds. If a chain happens to become oriented along (010), that is, at 45° with respect to the dimer rows, it can make many C–Ge bonds without being strained too much. Because the density of the bonds is high, such a chain stops locally the flow of surface steps and causes a $(10n)$ facet to be formed (Fig. 2d-f)[3]. The surface roughens, developing a characteristic pattern of ridges. The step flow is a natural consequence of high deposition temperatures and high H content: the steps move because surface Ge vacancies created by Ge sublimation or by H etching migrate to the steps edges.

Optimally, each surviving seed should be long but attached to Ge by rarely spaced bonds. Such seeds might coalesce without losing the information about the substrate orientation, and their weak interaction with the substrate would cause no excessive roughening.

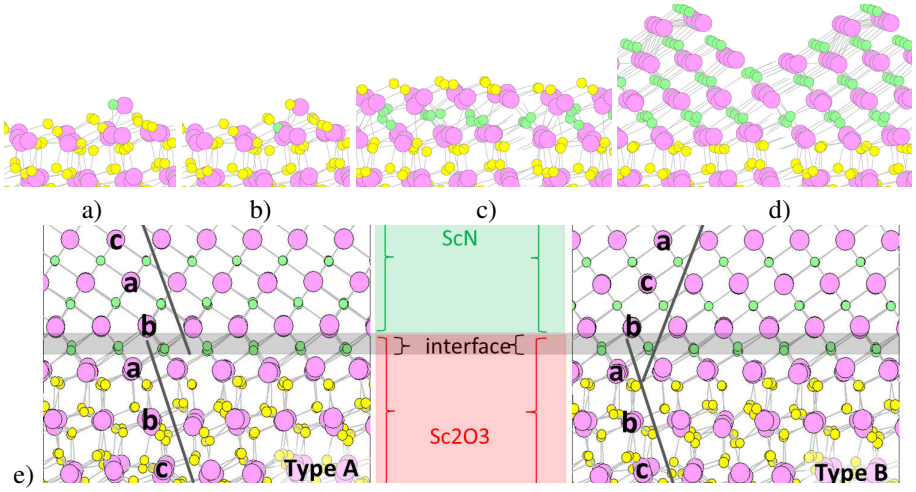

Figure 3. ScN(111) growth on Sc_2O_3(111). Sc is big and pink. (a-b) O-N exchange in ScN dimer. (c) O segregation. (d) Faceting. (e) Stacking. Interfacial O is substituted by N, which fills also the vacancy sites. The stacking in type-A is cab-abc, because abc-abc is in conflict with the interfacial anion sites inherited from Sc_2O_3.

4 ScN on Sc_2O_3

ScN(111) films have been deposited in an MBE chamber from N_2 plasma and atomic Sc[4]. Our experimental observations and theoretical calculations agree that there is no significant incorporation of N into Sc_2O_3 from N_2 plasma alone. The theoretical conclusion[4] follows from the energy balances and barriers computed for reactions of N_2 and N with the surface of Sc_2O_3 as compared to the energy carried by and the composition of the plasma. Yet N is found in Sc_2O_3 after the ScN film is grown. This N may become inserted during the initial phase of deposition, when ScN dimers form on the surface (Fig. 3a-b). At this stage, ScN dimers convert into ScO dimers and N may diffuse into Sc_2O_3. We have no theoretical evidence for direct intermixing of N and O between ScN and Sc_2O_3 layers.

From the dependence of X-ray photoelectron spectroscopy (XPS) O 1s signal on the ScN thickness we infer that O segregates to the surface of the growing film and is gradually removed from there by the plasma[4]. This is in line with the DFT prediction[4] that O at the Sc_2O_3/ScN interface is substituted by nitrogen and placed on top of the growing film (Fig. 3c). The ScN(111) internal dipole moment is compensated in this way. The energy barrier to remove this oxygen by N_2 plasma is lower than it is for the Sc_2O_3(111); this may explain the gradual disappearance of the O 1s XPS signal[4]. The internal dipole moment of oxygen-free ScN can be compensated by micro-faceting of the ScN(111) surface (Fig. 3d)[4].

One of the reasons why it is better to grow ScN on an oxide buffer than directly on Si is that Si/ScN develops twins, while Sc_2O_3/ScN does not. The twinning is due to the presence of two stacking sequences, of type A and B, that are possible in a (111) film with the rock-salt structure (Fig. 3e). According to DFT, the type B observed on Sc_2O_{30} in experiment (Fig. 3e, right) has the interface energy lower than that of type A by about 5 eV/nm^2. This is because of better structural matching for type B than for type A (Fig. 3e) and because the substrate is ionic: the electrostatic contribution to the total energy enhances the effect.

5 Vacancies and Oxygen in Si Bulk

The main difficulties associated with DFT calculations for vacancies and their clusters in Si is that these defects are not only electrically active but in addition they are a source of strong strain fields. This results in spurious long-range electrostatic and elastic interactions in the superlattice produced by periodic boundary conditions inherent to calculations with the plane wave basis set. On the other hand, this is to certain extent offset by the "soft" character of Si pseudopotentials: relatively small number of plane waves is needed, meaning that supercells consisting of many atoms can be treated. This makes Si vacancies a graceful system to investigate the finite-size effects caused by such interactions.

We investigated these effects in a systematic way[5], using supercells with Si lattice sites from 128 to 1458. We placed most emphasis on the energies of charge transition levels of the single vacancy (V_1) and its smallest clusters: the divacancy (V_2) and the trivacancy (V_3), for which well-established experimental DLTS data exist, and also on the formation energies of vacancy clusters V_n ($n \leq 11$) in the neutral charge state and in the charge state expected at high temperatures needed to work out the depth profile of oxygen precipitates, that is, for Fermi energies around the mid gap.

According to DLTS, V_1 has three deep donor levels (Fig. 4a). They are close to the valence band top, separated from one another by only about 40 meV, and arranged in the "negative U" fashion: the V_1^{++} and V_1^0 charge states are stable, but V_1^+ is not. The negative U property is reproduced by the least expensive calculations done with the reciprocal space sampling at Γ, but the absolute value of U diminishes with increasing separation between the vacancy images in the superlattice and the extrapolation to the dilute limit (infinite separation) reverses its sign, unless the results from the largest cell are ignored[5]. This may be because DFT places the band edges too close to one another. The valence band edge is too high in energy, so that the defect energies suffer from improper admixture of the band states. Improvement is achieved when the reciprocal cell is sampled at the L point of the Brillouin zone or when a hybrid functional (HSE06) is used in place of a semilocal (PBE) one. The calculations at L (in general, with k-points away from Γ) are more expensive. In such cases they can be done with the atomic positions optimised at Γ, so that the additional costs are acceptable. But changing the functional from semilocal to a hybrid one does affect the atomic forces: additional relaxation is needed. Moreover, hybrid calculations are resource-hungry. To overcome this, one can assume that the functional dependence of the transition state energies on the cell size is the same for hybrid and semilocal exchange-correlation. In this way, one can extrapolate to infinity the results obtained with only two cell sizes. We verified for V_1 that this works (Fig. 4b). It is probably so because this dependence is dominated by other factors than the spurious valence state admixture.

Our analysis of the vacancy clustering (Fig. 4c) shows that the stability of V_6 and V_{10} is kinetically enhanced[6]. For example, V_6 is created faster ($V_5+V_1 \rightarrow V_6$) than it is destroyed ($V_6+V_1 \rightarrow V_7$). This is true for uncharged defects and remains so when the presence of other charge states is taken into account.

Finally, we studied the trapping of interstitial oxygen by single vacancies and their clusters[6]. We found that the energy gained by trapping of an oxygen atom does not depend on the cluster size nor on the amount of oxygen already trapped until the free volume of the initial vacancy cluster is compensated by the volume of the interstitials. After that, the process continues, but with the energy gain halved (from 1.3 to 0.6 eV).

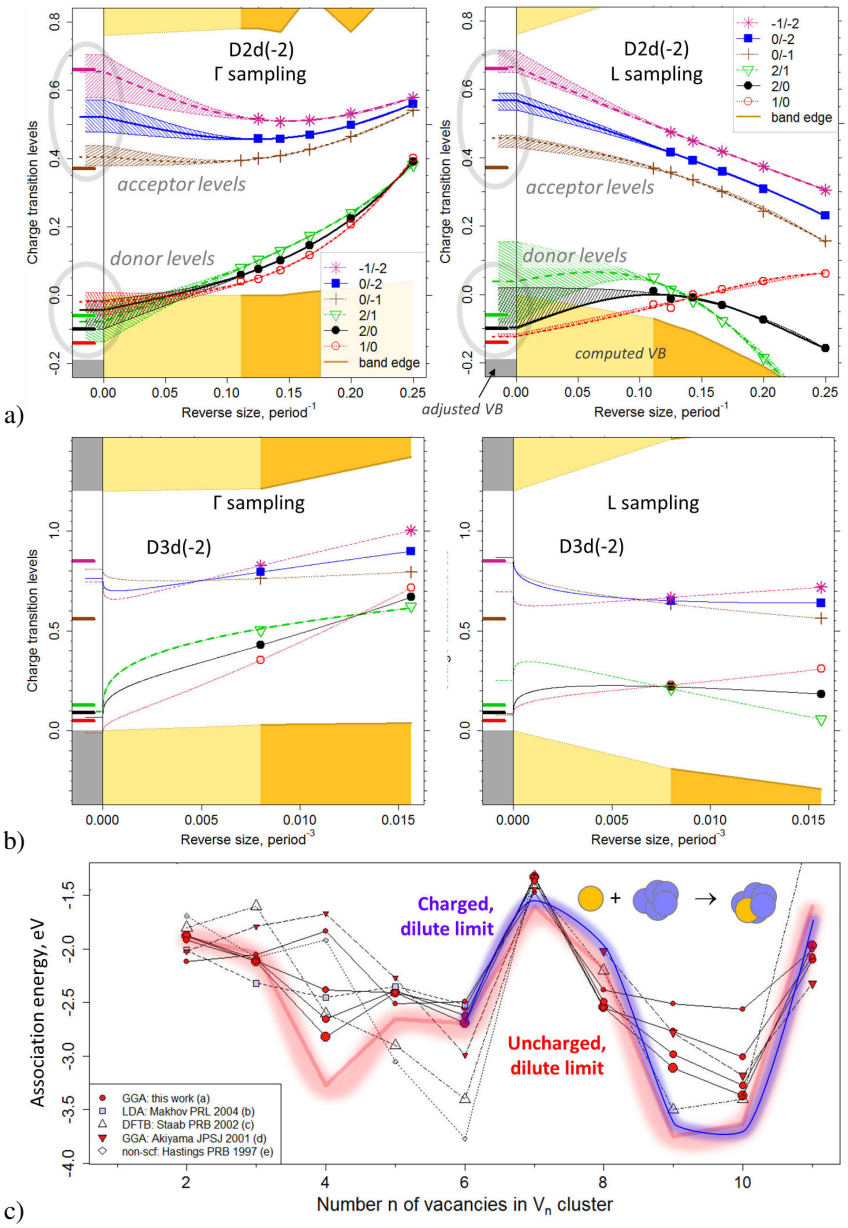

Figure 4. Finite size effects in Si V_n clusters. (a) Multipole extrapolation of PBE charge transition levels of V_1; DLTS data is shown on the left. The dashed area indicates the extrapolation inaccuracy; the solid lines are weighted means of extrapolations. (b) HSE06 levels of V_1. The extrapolation assumes the same exponent as that obtained with PBE data. (c) Association energies of vacancy clusters. Negative values mean energy gain when V_1 is attached. The charge states are those stable at the Fermi energy in mid gap. Adapted from Ref. 7.

6 Concluding Remarks

Ab initio DFT calculations coupled to experimental studies have been conducted to gain insight into a number of problems pertinent to materials development for silicon-compatible microelectronics. The nucleation and growth of graphene on Ge substrates from atomic carbon (MBE) and from hydrocarbon precursors (CVD) was modelled and the associated physical mechanisms were elucidated, including the mechanism of the interface layer formation between germanium and graphene during the MBE process and the faceting of the Ge(001) surface during the CVD process. Second, the growth of ScN films on Sc_2O_3 substrates by MBE was analysed starting from the exposure of the substrate to N_2 plasma and to Sc atomic beam, through the formation of the interface between Sc_2O_3 and ScN and the establishing of the stable stacking sequence, up to the removal by N_2 plasma of the oxygen segregated to the ScN surface, and the physical reason for the experimentally observed stacking sequence, dissolution of N in Sc_2O_3, and oxygen segregation was given. Third, the process of vacancy clustering and vacancy-assisted precipitation of oxygen in Si bulk was examined. Some of these results were systematically extrapolated to the dilute limit and the influence of such extrapolations on the interpretation of the experiments in terms of the raw computed data was discussed.

Acknowledgements

The authors gratefully acknowledge the computing time granted by the John von Neumann Institute for Computing (NIC) and provided on the supercomputer JURECA at Jülich Supercomputing Centre (JSC).

References

1. G. Lippert *et al.*, *Graphene on Ge(001) from atomic source*, Carbon **75**, 104, 2014.
2. J. Dabrowski *et al.*, *Understanding the growth mechanism of graphene on Ge/Si(001) surfaces*, Sci. Rep. **6**, 31639, 2016, and references therein.
3. M. Lukosius *et al.*, *Metal-Free CVD Graphene Synthesis on 200 mm Ge/Si(001) Substrates*, ACS Appl. Mater. Interfaces **8**, 33786, 2016, and references therein.
4. P. Sana *et al.*, *Growth Mechanism of ScN on Sc2O3 for GaN Integration on Si(111)*, J. Appl. Phys. **120**, 135103, 2016, and references therein.
5. J. Dabrowski and G. Kissinger, *Supercell-size convergence of formation energies and gap levels of vacancy complexes in crystalline silicon in density functional theory calculations*. Phys. Rev. B **92**, 144104, 2015, and references therein.
6. G. Kissinger *et al.*, *Ab Initio Calculations and Rate Equation Simulations for Vacancy and Vacancy-Oxygen Clustering in Silicon*, J. Crys. Growth **468**, 424, 2016.
7. J. Dabrowski and G. Kissinger, *Vacancies in silicon, formation of their complexes, and reactions between them*, 29th International Conference on Defects in Semiconductors (ICDS), Matsue, Japan 2017 (invited), `http://www.icds2017.org`.
8. P. Giannozzi *et al.*, *QUANTUM ESPRESSO: a modular and open-source software project for quantum simulations of materials*, J. Phys. Cond. Mat. **21**, 395502, 2009.